Imaging Scattered Seismic Energy in Alberta Oil Sands

Andrew V. Barrett*, Statoil Canada Ltd., Calgary, Alberta, Canada
AnBarr@Statoil.com

Summary

The objective of this presentation is to demonstrate the separation of the scattered energy image from the specular reflections over a 3D seismic survey to provide an estimate of the inhomogeneities along the reflecting horizons. Particular emphasis is given to issues related to oil sands in a SAGD operation.

Introduction

Inhomogeneities along a reflecting horizon scatter seismic energy. Inclined heterolithic stratigraphy (IHS) may have inhomogeneities which could serve as permeability baffles, allowing steam to pass in a SAGD operation. Some IHS may be homogeneous along its extent, serving as a uniform permeability barrier for steam. The purpose of migration is to move scattered energy to the position of the scatterer and to produce an accurate image of the reflector. However, specular reflections on a smooth reflector would result in an image at the same position as the image from the scattered energy. The scattered energy image is separated in this presentation from the specular reflection image to provide an estimate of the inhomogeneities along the reflecting horizons.

Kirchhoff PSTM was modified with the introduction of the concept of a differential migration time gather, where each trace in the gather represents a constant traveltime difference between the specular reflection traveltime and the computed traveltime from the recorded trace to the image trace. This new image gather space was used for parameter selection, testing, and evaluation of the existence and quality of scattering events. The final scattered energy migration was accomplished with appropriate tapers applied to the Kirchhoff migration operator, without producing the intermediate output of the differential migration time gather.

Theory and Method

The Kirchhoff integral is

$$U(\mathbf{x}) = \iiint_{\Sigma} R(\mathbf{x}_s,\mathbf{x}_r,t)\, G(\mathbf{x},\mathbf{x}_s,\mathbf{x}_r,t,v)\ \ dt\, d\mathbf{x}_s\, d\mathbf{x}_r$$

where $\mathbf{x}_s$ and $\mathbf{x}_r$ are the source and the receiver locations; $\mathbf{x}$ denotes an image point within the acquisition surface Σ; R is the recorded data; and G is the Green's function, relating the surface to the image point in terms of traveltime as well as compensating for amplitude changes along the raypath.

Introduce the change of variable $\tau = t - t_m$, where $t_m(\mathbf{x},\mathbf{x}_s,\mathbf{x}_r)$ is a reference time. In the case of time migration, t_m is taken to be the two way travel time to $\mathbf{x}$ from surface points having the same offset and azimuth as $(\mathbf{x}_s,\mathbf{x}_r)$, but with midpoint $\mathbf{x}$. So t_m is the minimum traveltime for that offset and azimuth to an image point at that depth, and τ is non-negative for flat reflectors. For depth migration t_m could be defined in the same manner, but not necessarily be non-negative, or it could be defined in some other manner. In this paper I am using time migration.

This results in a modification to the Kirchhoff integral

$$U(\mathbf{x}) = \iiint_{\Sigma} R(\mathbf{x}_s,\mathbf{x}_r, \tau+t_m)\, G(\mathbf{x},\mathbf{x}_s,\mathbf{x}_r, \tau+t_m,v)\, d\mathbf{x}_s\, d\mathbf{x}_r\, d\tau$$

The reason I did this is so that the inner integrals are over the acquisition surface, and we are left with a function of , which can be implemented as a binned variable producing traces analogous to offset image gathers:

$$U_\tau(\mathbf{x}) = \iint_{\Sigma} RG\, d\mathbf{x}_s\, d\mathbf{x}_r$$

I am calling the set of all image traces U_τ for a set of binned values of τ the “differential migration time gather”.

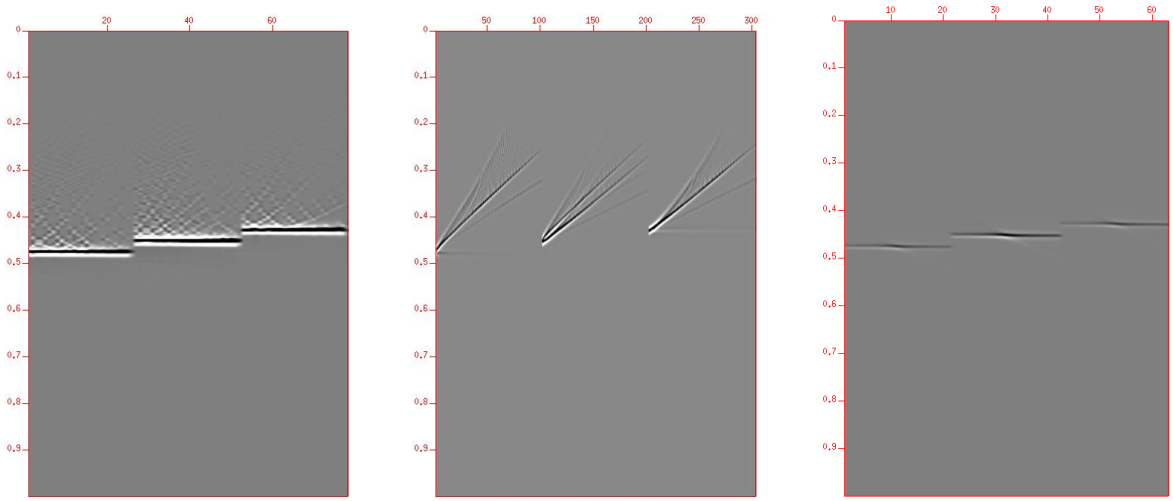

Figure 1: Three migrated gathers: (left) offset gathers, (middle) differential migration time gathers, (right) velocity scan gathers.

Because the computed traveltime, as well as compensation for the effects of dispersion, for the longer and more oblique travel path of the scattered energy is not as accurately known as for the specular reflection, the Green’s function in the Kirchhoff migration was modified from the standard delta function to a short, white operator adaptively designed to optimally match a pilot image.

Provision was made in the PSTM for orthorhombic isotropy in the velocity field, although accurate estimation of the azimuthal component is difficult and the estimate made from offset-vector tile migration did not significantly alter the imaging in our case. Only vertical transverse isotropy (VTI) was used, with an effective η incorporating both the effects of the anisotropy and the curved raypaths of the depth-dependent velocity.

Examples

A prestack Kirchhoff time migration module which outputs a set of traces at each surface position was written incorporating the usual software design. Field data traces are input to the module in any order. The spatial and temporal extents of the output imaged canvas are specified by user parameters. The

set of traces in the differential migrated time domain is also specified, as are offset image bins, if requested As the traces are read, the partially migrated images are gradually accumulated. Partial image datasets are periodically output, for disaster recovery. Parallelization may be accomplished either by partitioning the input dataset, by partitioning the output canvas, or some combination of the two.

I will show two examples: first a set of synthetic datasets, secondly the results on an oil sands 3D survey.

For the synthetic datasets I take a single, slightly dipping reflector, and insert breaks as varying intervals. In all cases the reflector extends for 1000m. The four configurations with inhomogeneities introduced along the reflector are:

Model A: Continuous reflector.
Model B: Every 100m, place a 20m gap in the reflector.
Model C: Every 20m, place a 10m gap in the reflector.
Model D: Every 10m, place a 5m gap in the reflector.

Upon creating 2.5D prestack datasets and migrating in the usual PSTM, the resulting full migrated images are:

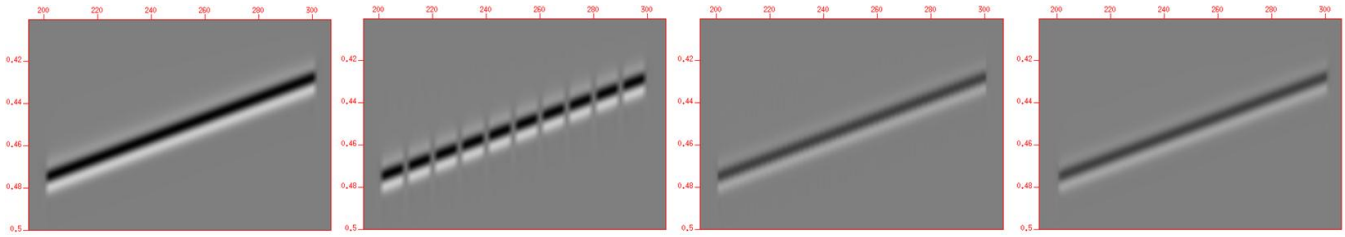

Figure 2: Full migration of datasets created from Models A-D.

However, when the migration is modified so that only the larger values of the differential migration time are included in the imaging, the resulting images are:

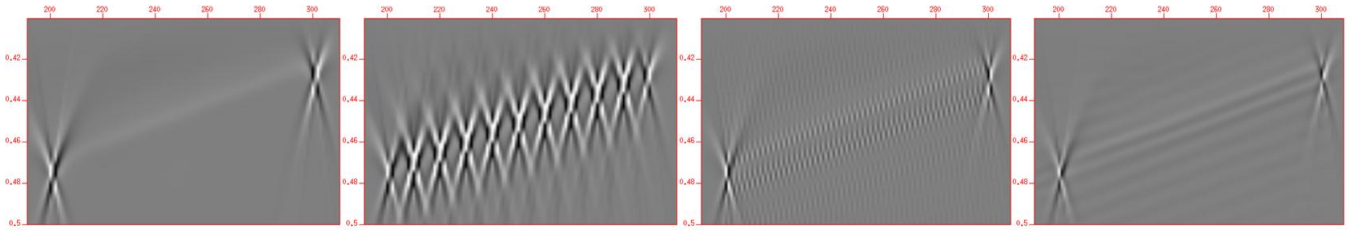

Figure 3: Scattered energy image of datasets created from Models A-D.

Although models A, C, and D are essentially indistinguishable in the full migrated image, the scattered energy images are quite distinct.

Next I ran a full migration and a scattered energy migration on a dataset acquired over KOSP (Kai Kos Dehseh Oil Sands Partnership) oil sands property in northern Alberta. Below is one piece of those images:

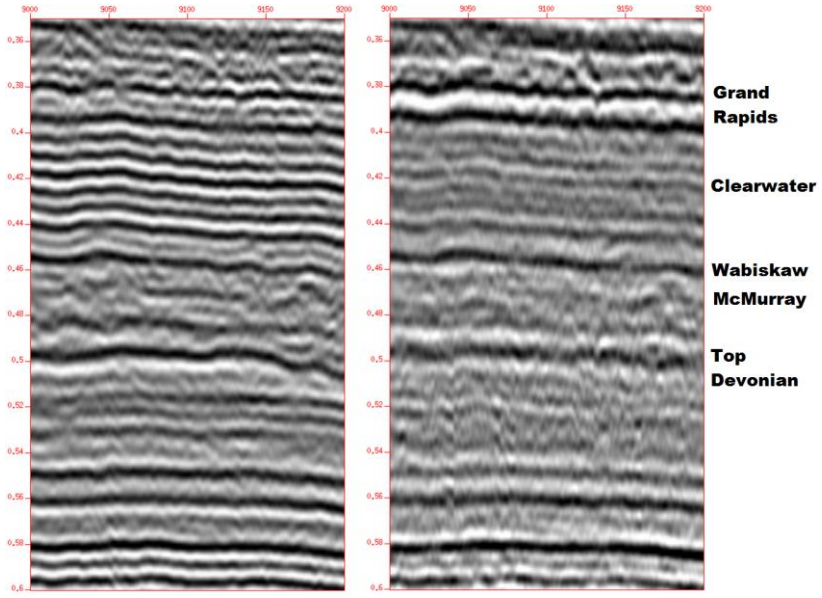

Figure 4: Full migrated image (left) and scattered energy image (right) in oil sands area.

The obvious difference is that Grand Rapids formation shows much greater relative scattered energy than the Clearwater formation. This is consistent with the relative inhomogeneity of these formations from cores. The real item of interest is differences in scattered energy reflectivity within the McMurray formation, which we hope would indicate a level of inhomogeneity of permeability barriers influencing the transmission of steam in our SAGD operations.

Conclusions

The principal objective of this method is to decompose recorded energy into the energy which reflects from smooth surfaces, and the energy which is scattered by rugose interfaces, event terminations, and other inhomogeneities in the subsurface. Rather than relying on imperfect migration schemes to image these inhomogeneities, we attempt to partition the migration result to separately image these two sorts of recorded energy.

The software works, and has been demonstrated here on a simple synthetic model. Examples of images through a 3D survey in the oil sands show interesting differences between the scattered energy and full image. Interpretation continues. This method is a result from a research program at Statoil, and does not represent current best practice in Statoil.

Acknowledgements

Thank you to the KOSP partners, Statoil and PTTEP, for allowing me to present this work, to Ion Geophysical for the pre-migration processing of the data, and to my lovely wife, Claudia, for encouraging me along the way.

References

Kozlov, E., N. Baransky, E. Korolev, A. Antonenko, and E. Koshchuk, 2004, Imaging scattering objects masked by specular reflections: 74th Exposition and Annual International Meeting, SEG, Expanded Abstracts, 1131-1134.

Khaidukov, V., E. Landa, and T. J. Moser, Diffraction imaging by focusing-defocusing: An outlook on seismic superresolution, **Geophysics**, November 2004 , **69**:6, 1478-1490.

Fomel, Sergey, Evgeny Landa, and M. Turhan Taner, Poststack velocity analysis by separation and imaging of seismic diffractions, **Geophysics**, November-December 2007, **72**:6, U89-U94